Human Molecular Genetics, 2011, Vol. 20, No. 8 **1633–1642**
doi:10.1093/hmg/ddr040
Advance Access published on February 9, 2011

Premature death and neurologic abnormalities in transgenic mice expressing a mutant huntingtin exon-2 fragment

Andrew T.N. Tebbenkamp[1], Debbie Swing[2], Lino Tessarollo[2] and David R. Borchelt[1,*]

[1]Department of Neuroscience, SantaFe HealthCare Alzheimer's Disease Research Center, McKnight Brain Institute, University of Florida, 100 Newell Dr, Rm. L1-100, Gainesville, FL 32610, USA and [2]Mouse Cancer Genetics Program, Neural Development Section, National Cancer Institute, Frederick, MD 21702, USA

Received December 9, 2010; Revised December 9, 2010; Accepted January 27, 2011

Huntington's disease (HD) is a fatal neurodegenerative disease characterized pathologically by aggregates composed of N-terminal fragments of the mutant form of the protein huntingtin (htt). The role of these N-terminal fragments in disease pathogenesis has been questioned based in part on studies in transgenic mice. In one important example, mice that express an N-terminal fragment of mutant htt terminating at the C-terminus of exon 2 (termed the Shortstop mouse) were reported to develop robust inclusion pathology without developing phenotypic abnormalities seen in the R6/2 or N171-82Q models of HD, which are also based on expression of mutant N-terminal htt fragments. To further explore the capacity of mutant exon-2 htt fragments to produce neurologic abnormalities (N-terminal 118 amino acids; N118), we generated transgenic mice expressing cDNA that encodes *htt* N118-82Q with the mouse prion promoter vector. In mice generated in this manner, we demonstrate robust inclusion pathology accompanied by early death and failure to gain weight. These phenotypes are the most robust abnormalities identified in the R6/2 and N171-82Q models. We conclude that the lack of an overt phenotype in the initial Shortstop mice cannot be completely explained by the properties of mutant htt N118 fragments.

INTRODUCTION

Huntington's disease (HD) is a genetic, fatal, neurodegenerative disorder with symptoms that include movement, cognitive and psychiatric abnormalities (reviewed in 1). The HD mutation is an expansion of a polyglutamine (polyQ) tract in the first of 67 exons of the huntingtin (*htt*) gene; expansion of the repeat beyond 40 consecutive glutamines invariably causes the disease (2). Post-mortem analysis of human HD brains shows marked widespread atrophy, with notable cell loss in the striatum and cortex (3,4). Neurons throughout the central nervous system develop cellular pathology that consists of ubiquitinated, nuclear and cytoplasmic inclusions (5,6). This inclusion/aggregate pathology has also been observed in transgenic mice (7–9), knock-in mice (10–12) and numerous cell culture models (13–16). The pathologic inclusions are composed of a small N-terminal cleavage product of mutant htt that is thought to terminate N-terminal to amino acid 115 [this fragment has been referred to as cleavage product-A (Cp-A) or cleavage product-1] (16–19). Many studies have documented that N-terminal fragments of mutant htt are more prone to aggregate and are more toxic to cultured cells than full-length mutant htt (13,20,21).

Studies of mouse models of HD have provided evidence that favored the view that N-terminal fragments of mutant htt could be mediators of toxicity. The R6/2 mouse model expresses the first exon of human *htt* (amino acids 1–90) with ~140Q and exhibits inclusion pathology (7), accompanied by brain atrophy (22), motor deficits (23), a failure to thrive and premature death (24). Similar phenotypes were observed in mice expressing the first 171 amino acids of htt with 82 glutamine repeats (8,25). Notably, the N171-82Q fragment is cleaved to produce a small Cp-A-like fragment that ultimately produces intranuclear and cytoplasmic aggregates (17). The YAC128

*To whom correspondence should be addressed. Tel: +1 3522739664; Fax: +1 3523928347; Email: borchelt@mbi.ufl.edu

and BACHD mice express full-length htt (3144 amino acids, 67 exons) but ultimately develop inclusion pathology composed of small htt N-terminal fragments (26,27). Additionally, mice with an expanded polyQ knocked-in to their endogenous *htt* allele develop inclusion pathology containing smaller N-terminal fragments of mutant htt (19). Neither the yeast artificial chromosome (YAC), bacterial artificial chromosome, nor knock-in models show abbreviated lifespans. A recent comparison of knock-in (*Hdh*Q150) and R6/2 mice showed that the behavioral impairments and aggregate deposition of the *Hdh*Q150 mice were similar to those of the R6/2 but developed later and progressed more slowly (28). Collectively, these studies suggest a linkage between the generation of N-terminal cleavage products of mutant htt, inclusion pathology and neurologic toxicity.

However, in 2005, Slow *et al*. (9) described transgenic mice (termed 'Shortstop' mice) expressing the first two exons (amino acids 1–118) of human htt with 120Q that developed widespread inclusion pathology but exhibited no behavioral abnormalities, normal lifespans and no brain atrophy. The Shortstop mice were created when a fragment of a mutant *htt* YAC, which encompasses the *htt* promoter, the first two exons and part of the second intron, integrated in a manner to produce a truncated protein. The shortstop fragment is produced because the second intron contains an in-frame stop codon just downstream of the 3′ splice donor site of exon 2 with a cryptic poly-adenylation site further downstream. The resulting mRNA transcript codes for an htt fragment that would correspond to the first 118 amino acids of normal *htt* (23Q base). Because the same YAC that was injected to produce Shortstop mice has been used to produce mice that express full-length mutant htt, which develop motor function deficits and brain atrophy, Slow *et al*. (9) suggested that the N118 fragment of mutant htt may be less toxic than full-length htt. The N118 shortstop fragment is similar in length to, but not identical to, the aforementioned Cp-A fragment that appears to produce the inclusion pathology of HD. The Cp-A fragment terminates between residues 105 and 114 and thus is slightly shorter than the shortstop fragment (16,17). In cultured cell models of mutant htt toxicity, expression of N118-120Q was reported to produce less activation of caspase 3 than expression of N171-82Q constructs, suggesting that the N118 fragment is less toxic (21). Notably, the N171-82Q fragment is cleaved to produce a Cp-A-sized fragment, which produces inclusions in mice and cell culture models (17). Thus, whether the specific length of the N118 fragment reduced its toxicity was in question.

In the present study, we sought to further investigate the relative toxicity of the shortstop htt fragment in transgenic mice. In designing the experiment, we chose to construct *htt* N118 cDNA genes with 82 glutamines to express via the mouse PrP.Xho vector so that the new mice could be compared with existing N171-82Q mice (8). We found that mice expressing N118-82Q via the mouse PrP.Xho vector exhibit pathological and behavioral phenotypes similar to the R6/2 and N171-82Q mice. While these data do not directly indicate that aggregates themselves are pathogenic, they support the body of the literature showing that truncated forms of mutant htt produce neurological abnormalities *in vivo*. We conclude that the basis for the lack of overt phenotypes in the Shortstop mice described by Slow *et al*. (9) is not explained by the specific length of the fragment.

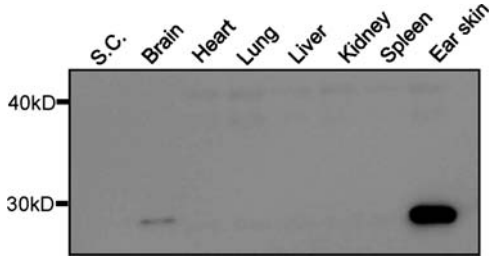

Figure 1. The K14-eGFP transgene is expressed in the skin and at low levels in the brain. Each lane contains 10 μg of detergent soluble protein as described in Materials and Methods. Immunoblots were probed with anti-GFP antibody clone mJL-8 and visualized by chemiluminescence on a Fuji imaging system. Spinal cord (S.C.). The image shown is representative of three replications.

RESULTS

Generation of transgenic mice

In creating the N118-82Q mice, we developed a means to visually genotype transgenic animals. We engineered a reporter transgene, encoding enhanced green fluorescent protein (eGFP), that was designed to be co-injected with *htt* N118-82Q transgene constructs. The eGFP reporter was constructed by inserting the cDNA into a vector harboring a keratin-14 (K14) promoter to drive expression of eGFP in skin. The K14 vector was created by removing the promoter element of the MoPrP.Xho vector and replacing it with a 2 kb fragment of the human *keratin-14* gene (Supplementary Material, Fig. S1). A strategy similar to this approach was used previously to produce a vector that can be regulated by tetracycline analogs (29). Previous studies have shown that co-injection of two independent transgenes results in co-integration of the transgenes at a single locus (30,31). In our experience, the two transgenes are so closely integrated that recombination to segregate the genes virtually never occurs.

To test the toxicity of mutant N118 htt fragments, we produced cDNA encoding *htt* N118 with an 82Q repeat (N118-82Q) and inserted the cDNA into the MoPrP.Xho vector for embryo injection (32). N118-82Q encodes the first two exons of *htt*; amino acid numbering uses a 23Q base (NCBI Reference Sequence: NM_002111). This construct was co-injected with the K14-eGFP construct (mice henceforth referred to as HD118-eGFP). In parallel, we generated strains of mice that harbor the K14-eGFP construct alone and mice that were co-injected with K14-eGFP and Mo.PrP-N171-82Q constructs (mice henceforth referred to as HD171-eGFP). These two constructs provided negative and positive controls, respectively. The Mo.PrP-N171-82Q construct is identical to a construct used previously to produce HD-N171-82Q line 81 mice (8), to which we compare the new lines of mice that are now described. Using goggles fitted with the appropriate filters to visualize eGFP expression, we could reliably distinguish transgenic mice from non-transgenic (NTg) mice. To illustrate, we captured an image of newborn mice in a Fuji imager (Supplementary Material,

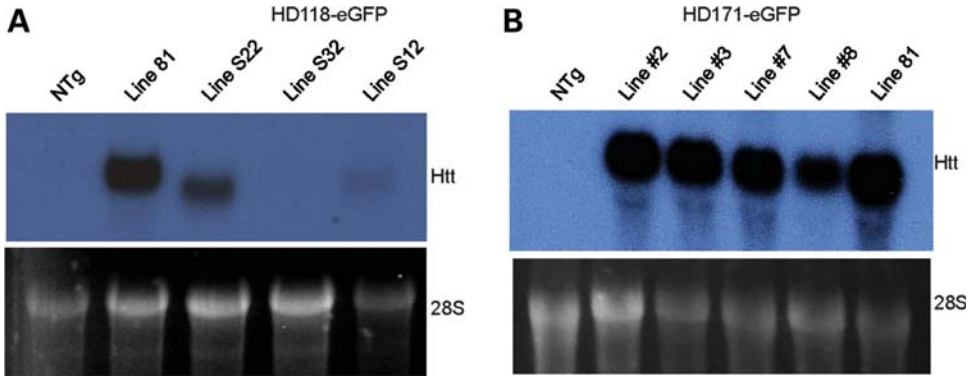

Figure 2. Northern blot analysis of transgene mRNA. (**A**) The top portion of the figure shows the level of N118-82Q mRNA in different lines of mice (S12, S22 and S32). NTg and N171-82Q (line 81) serve as relative controls ranging from no expression (NTg) to maximum achieved (line 81). (**B**) The top portion of the figure shows the level of N171-82Q mRNA in new lines of HD171-eGFP mice (lines #2, #3, #7 and #8). The bottom portion of each figure shows the UV image of the formaldehyde/agarose gel to demonstrate the levels of 28S RNA. The membranes were probed with radiolabeled *htt* cDNAs as described in Materials and Methods. The image shown is representative of two replications.

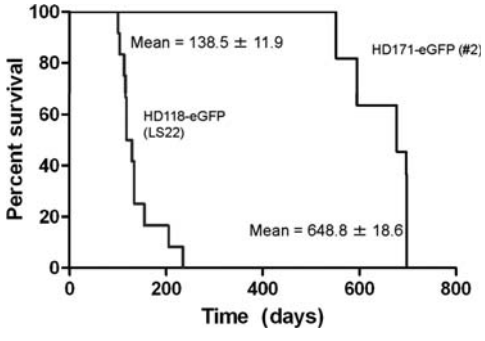

Figure 3. Life expectancy of HD118-eGFP and HD171-eGFP mice. A Kaplan–Meier plot of line S22 (blue line) shows that this line of mice dies prematurely. After ~100 days, the percentage of mice that survive gradually decreases (mean = 138.5 ± 11.9 days, SEM, $n = 12$). Mice from HD171-eGFP line #2 (black line) live substantially longer (mean = 648.8 ± 18.6 days, SEM, $n = 11$).

Fig. S2). The expression of eGFP persists into adulthood and is most visible in ears, paws and tail skin. To determine whether the eGFP was only expressed in skin, we performed immunoblot analysis of various tissues. As expected, eGFP was easily detected in the skin from an ear biopsy (Fig. 1). No other tissue expressed eGFP except for a weak signal in brain lysates. In sagittal brain sections from several independent strains of mice harboring the K14-eGFP transgene, eGFP was detectable in multiple regions of the brain with the highest level usually found in the forebrain and cerebellum (Supplementary Material, Fig. S3). However, we did note some variability within mice of the same strain as the intensity of eGFP in different structures varied between mice. Mice harboring the K14-eGFP transgene alone appeared normal throughout their lifespan (out to >530 days at the time of writing). We note that numerous lines of mice expressing fluorescent proteins in the central nervous system (CNS) have been generated and reported to be free of abnormalities (33–35). Thus, we were confident that some expression of the eGFP reporter in the brain would be unlikely to affect the outcome of our study of N118-82Q expression while simultaneously allowing rapid identification of transgenic mice.

Identifying HD118-eGFP founders

In generating HD118-eGFP mice, we initially identified 10 founders that harbored the *htt* transgene, detected in genomic DNA from tail-biopsy, and they all expressed varying levels of eGFP in skin. Several founders that were among those with the most fluorescent skin died prematurely before producing offspring. However, we were able to establish three lines to breed cohorts for downstream analysis. Northern blot analyses of brain RNA were performed to compare relative expression levels of transgene mRNA among these new lines of mice and to compare the levels to our previously established HD-N171-82Q line 81 mice (8), which do not harbor the K14-eGFP transgene. Of the three breeding lines of HD118-eGFP mice, the line designated S22 expressed the highest level of htt; however, the level was ~50% lower than that of HD-N171-82Q line 81 mice (Fig. 2A). Immunoblot analyses of brain lysates from young HD118-eGFP mice confirmed expression of the N118-82Q protein in the brain and that line S22 expressed the highest levels (Supplementary Material, Fig. S4). Lines S32 and S12 were terminated due to low expression levels. Northern blots were also performed to determine the levels of transgene mRNA in the brains of the newly generated HD171-eGFP mice. In all cases, the level of transgene mRNA in the brains of the HD171-eGFP mice was at least 50% lower than that of the HD-N171-82Q line 81 mice (Fig. 2B). We chose to further evaluate three lines of HD171-eGFP mice, designated HD171-eGFP#2, #3 and #7. HD171-eGFP#8 mice were discontinued due to low expression.

Behavioral phenotype of HD mice

HD118-eGFP line S22 mice exhibited an early failure to thrive and premature death at 138.5 ± 11.9 days (SEM; $n = 12$) (Fig. 3). Two mice lived almost twice as long as the majority, which may be a result of loss of copy number (blue line of Fig. 3, >200 days). The new lines of HD171-eGFP mice developed phenotypes similar to the line S22 mice, but at much later ages. The HD171-eGFP#2 mice have lifespans of about 648.8 ± 18.6 (SEM; $n = 11$) days of age (Fig. 3). The

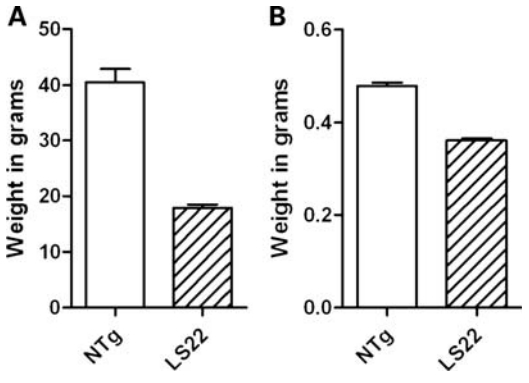

Figure 4. HD118-eGFP mice show reduced body and brain weights. (**A**) Age-matched NTg (white bars) body weight was 40.54 ± 2.39 g ($n = 7$), more than twice as much as line S22 mice (lined bars) at end-stage, 17.88 ± 0.64 g ($n = 7$, unpaired t-test $P < 0.0001$). (**B**) Average brain weight for NTg mice immediately after harvesting was 0.479 ± 0.007 g ($n = 7$). Line S22 mice had a significantly reduced brain weight at 0.360 ± 0.004 g ($n = 4$, unpaired t-test $P < 0.0001$).

HD171-eGFP#3 and #7 mice were established as lines only recently and we have limited data on life expectancy. We have observed HD-related abnormalities and early death in the HD171-eGFP#3 mice at about 12 months of age. The founder for HD171-eGFP#7 mice died at 8 months of age. The general appearance of the HD171-eGFP#2 mice was similar to that of the previously described HD-N171-82Q line 81 mice (8) in that observed phenotypes included failure to gain weight and hypoactivity towards the end of life expectancy.

Similar to the previously described HD-N171-82Q line 81 mice, the HD118-eGFP line S22 mice failed to gain weight (Fig. 4A). Line S22 mice were indistinguishable from their NTg littermates until weaning stage (~28 days), at which point they began to gain less weight. By end-stage, transgenic line S22 mice weighed less than half of their NTg littermates (NTg, 40.54 ± 2.39 g, $n = 7$ versus S22, 17.88 ± 0.64 g, $n = 7$). End-stage was generally defined by criteria similar to what we use for the HD-N171-82Q mice, which included decreased body weight and failure to ambulate upon prodding (Supplemental Information, Video S1). Brains from end-stage line S22 mice weighed significantly less than NTg littermates (Fig. 4B, NTg, 0.479 ± 0.007 g, $n = 7$ versus S22, 0.360 ± 0.004 g, $n = 4$).

Neuropathology of HD118-eGFP mice

One of the pathologic hallmarks of human HD is cytoplasmic and intranuclear inclusions that are immunoreactive to both htt and ubiquitin (5,6). To assess whether line S22 mice recapitulated this inclusion pathology, we performed immunohistochemistry on brain sections and compared those results to line 81 mice expressing N171-82Q and the HD171-eGFP#2 mice. As expected, the brains of S22 mice showed abundant inclusion pathology in multiple brain structures (Fig. 5). In comparison to the pathology of HD-N171-82Q line 81 mice and HD171-eGFP#2 mice, the inclusions in the brains of the line S22 mice were larger, more heterogeneous in size and more obvious or frequent in cytosol (Fig. 6). The inclusions in lines 81 and HD171-eGFP#2 were of approximately the same size and almost exclusively in the nucleus (Fig. 6A and B). In the HD118-eGFP mice, extranuclear inclusions were more frequent and obviously larger (Fig. 6C). In all three cases, inclusions were usually immunoreactive for ubiquitin (Fig. 6). We also analyzed the brain pathology of mice from lines S12 and S32, and of the three founders that reached end-stage before reproducing. No pathology was evident in mice from lines S12 and S32 (Supplementary Material, Fig. S5), which express very low levels of transgene mRNA. However, the brains of the three founders (designated S23, S31 and S43) that showed early symptoms also showed inclusion pathology with features similar to the line S22 mice (Supplementary Material, Fig. S5).

DISCUSSION

In the present study, we have examined whether an N-terminal fragment of htt that terminates at residue 118 with 82 consecutive glutamines produces neurologic abnormalities when expressed in the brains of transgenic mice. Several animals expressing this transgene failed to thrive and died before breeding. However, we were able to establish one line of breeding animals that express the *htt* N118-82Q transgene at levels that approach that of previously described HD-N171-82Q line 81 mice (8). To ease the identification of these new transgenic animals, we co-injected the PrP-N118-82Q transgene construct with a K14-eGFP transgene construct, which expressed eGFP at high levels in skin. The phenotypes of these HD118-eGFP mice were generally identical to what has previously been described in HD-N171-82Q mice (Table 1) (8). Overt phenotypes included failure to gain weight, poor grooming, hypoactivity and premature death. In previous studies of HD-N171-82Q line 81 mice, we have described modest to moderate deficits in the ability to perform rotarod tasks (8,25). Because the rotarod deficits in the HD-N171-82Q line 81 mice are relatively modest, we chose to focus on the most robust phenotypes, which include early death, failure to gain weight, brain atrophy and inclusion pathology. Pathologically, the HD118-eGFP mice were similar to the HD-N171-82Q mice in that there was no overt evidence of neurodegeneration or cell loss, but there was a significant reduction in brain weight indicating general atrophy. Neurons throughout the brain contained htt and ubiquitin immunoreactive inclusion pathology. A subtle difference between the HD118-eGFP and HD-N171-82Q mice was that in the HD118-eGFP mice the inclusions were generally larger, more heterogeneous in size and more visible in neuropil. Overall, we conclude that expression of a mutant htt fragment that encompasses the first two exons of *htt* produces phenotypes similar to our previously described HD-N171-82Q line 81 mice (8) and the R6/2 model of HD (24).

In generating the N118-82Q mice, we employed a new technology in which we co-injected the *htt* transgene construct (PrP-N118-82Q) with a construct for expression of eGFP in skin (K14-eGFP). Although the eGFP was highest in skin, we did observe some expression of eGFP in the brain. In parallel to generating the HD118-eGFP mice, we produced lines

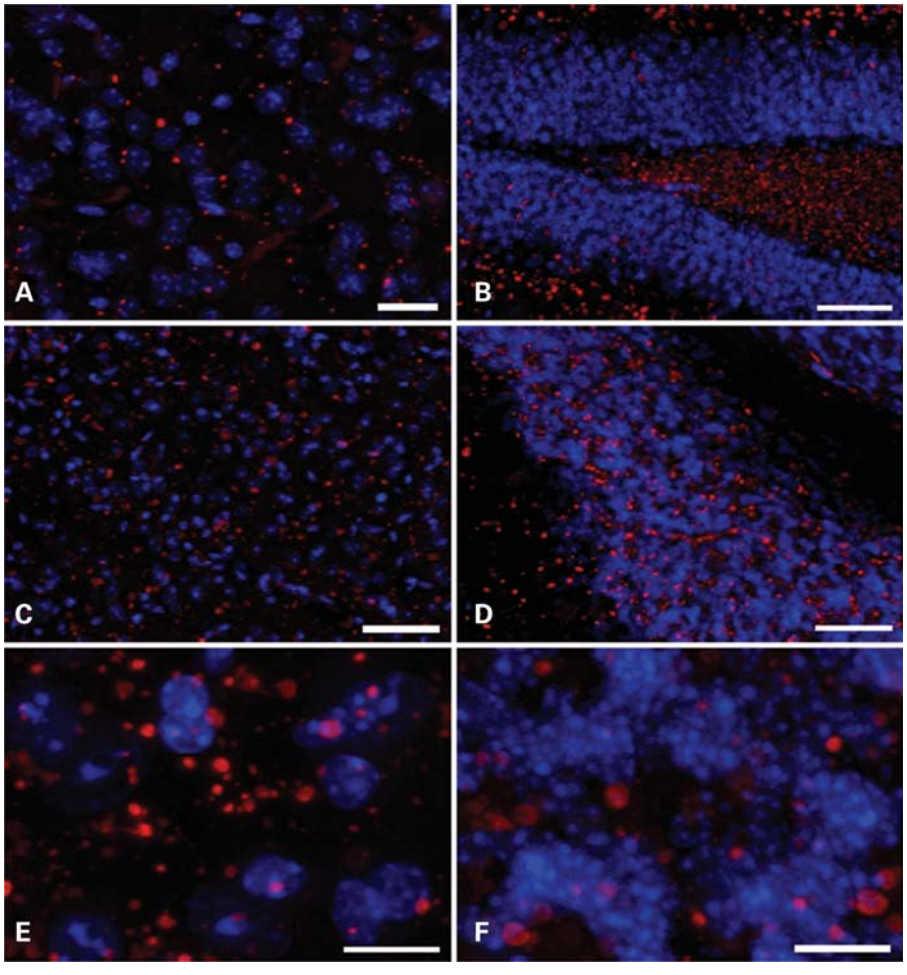

Figure 5. Inclusion pathology was observed in many brain regions in end-stage HD118-82Q line S22 mice. Htt inclusions (2B4 antibody, red) are seen in intra- and extra-nuclear compartments in the striatum (**A**), hippocampus (**B**), cortex (**C**) and cerebellum (**D**). (**E**) and (**F**) show the cortex and cerebellum, respectively, at higher magnification revealing the heterogeneous size and location of htt inclusions. Scale bars for (A–F) are as follows (in μm): 20, 50, 50, 50, 10 and 10. Nuclei are stained blue by DAPI.

of mice that were co-injected with PrP-N171-82Q and K14-eGFP constructs. All of these mice were compared with a previously generated line of mice that harbor the same PrP-N171-82Q construct used in the co-injection studies described here. The two new lines of HD-N171-82Q + eGFP mice we describe here (HD171-eGFP#2 and HD171-eGFP#3) show much longer life expectancies when compared with the original HD-N171-82Q line 81 mice. The difference in time to death between the two HD171-eGFP lines of mice and the HD-N171-82Q line 81 mice can be explained by the level of mutant htt expression. The levels of htt transgene mRNA in the HD171-eGFP lines was observed to be 30–50% lower than that of the line 81 mice. Although the levels of htt mRNA in the HD118-eGFP mice were comparable with the HD171-eGFP mice, the lifespan of the HD118-eGFP mice was considerably shorter than all of the lines of the HD171-eGFP lines of mice we produced. Thus, we conclude that the N118-82Q fragment is more toxic than the N171-82Q fragment.

Our original impetus in generating the HD118-eGFP mice we describe here was a report by Slow *et al*. (9) that described mice that were transgenic for a fragment of human genomic DNA derived from a YAC of the mutant *htt* gene. Upon integration, most of the coding sequence of *htt* was lost such that only the first two exons with a portion of the downstream intron were integrated in the genome. This DNA fragment is transcribed to produce an mRNA that in turn produces an N-terminal fragment of mutant (120Q) human *htt* that encompassed the first two exons, which equates to a termination at amino acid 118. A line of mice was developed and examined that was termed the Shortstop mouse (9). In contrast to the HD118-eGFP mice we describe here, the Shortstop mouse does not exhibit premature death or any other disease-associated phenotypes (Table 1) (9). The Shortstop mice were originally compared with mice harboring a YAC of the entire human *htt* gene with the same length repeat expansion (YAC128 mice). The YAC128 mice show motor deficits, reduced striatal volume and reduced brain weight by 12 months of age (9). In comparison to the YAC128 mice, the Shortstop mice show none of these phenotypes.

In comparing our new HD118-eGFP mice and the Shortstop mice, there are obvious differences in the way the mice were

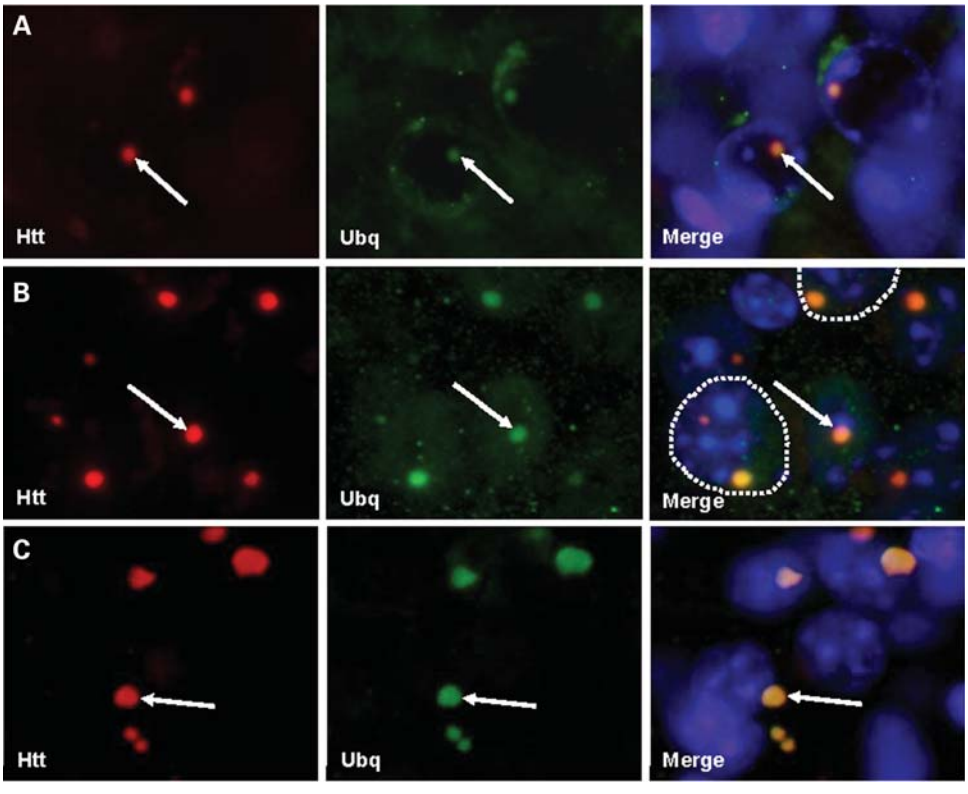

Figure 6. Comparison of htt inclusion pathology in HD-N171-82Q line 81, HD171-eGFP#2 and HD118-eGFP line S22 mice. (**A**) Brain sections from HD-N171-82Q line 81 mice show htt inclusions (left, red) are ubiquitinated (middle, green) and intranuclear (right, merged with DAPI). (**B**) Brain sections from line HD171-eGFP#2 mice show nearly identical htt/ubq intranuclear pathology. In some cases, nuclear borders are indicated with dashed white lines. The arrows in (A) and (B) indicate a typical inclusion. (**C**) HD118-eGFP line S22 brains also exhibit htt inclusions that are ubiquitinated (left and middle panels, respectively). However, it is common to observe inclusions outside of the nucleus, as indicated by the arrow (right panel).

Table 1. Summary of four transgenic HD mouse models

Mouse lines	Aggregates			Premature death?	Reduced weight	
	Size	Location	Ubq (+)		Body	Brain
N171-82Q line 81	Small	Nucleus	Yes	~6 months	Yes	Yes
N171-82Q + eGFP line HD eGFP #2	Small	Nucleus	Yes	~20 months	N/D	N/D
Shortstop	Small	Nucleus	N/D	No	N/D	No
N118-82Q line S22	Small, medium, large	Nucleus, cytoplasm	Yes	~4 months	Yes	Yes

N/D, not detected, measured.

produced that could explain the different outcomes. One obvious difference is the promoters used to drive the mutant *htt* transgenes. The Shortstop mouse is driven by 25 kb of upstream human *htt* sequence (9,36). If faithfully regulated in the mice, this transgene would be expressed beginning at embryonic day (E) 6.5 in the epiblast, at ~E8.5 in embryonic and extra-embryonic mesoderm (37), and throughout the CNS by E10 (38). The prion promoter, used to drive *htt* cDNA in our mouse models of HD, is activated throughout the CNS in all cell types by E13.5 (39). Because the prion promoter is activated later than the *htt* promoter, it is difficult to conclude that early developmental expression of N118-82Q in our HD118-eGFP mice produced some abnormality that induced the observed phenotypes. However, it remains very possible that differences in the distribution of gene expression accounts for the observed differences. For example, expression of an exon-1 fragment of mutant htt specifically in forebrain produces widespread inclusion pathology, but the authors did not report evidence of weight loss or abbreviated lifespans (40). Thus, it is quite possible that expression of mutant htt in a particular subset of neurons or in a particular visceral tissue is required to induce the phenotypes observed in the HD118-eGFP, HD-N171-82Q and R6/2 mouse models.

In regard to expression in visceral tissues, abnormalities in the transcriptional regulation of uncoupled protein 1 in brown fat have been implicated in contributing to the early death of the HD-N171-82Q and R6/2 models by disturbing thermoregulation (41). Notably, transgenic mice harboring a mutant human *htt* YAC with 72Q repeats mice do not show such abnormalities (41) despite the presence of widespread inclusion pathology composed of N-terminal fragments of mutant htt that are similar to the R6/2 and HD-N171-82Q

models (36). The Shortstop mice would be expected to have a pattern of expression similar to that of the YAC72 mice. Thus, it seems likely that differences in the pattern of transgene expression between the Shortstop and the HD118-eGFP mice could underlie the observed differences in phenotypes.

Another possible explanation for the different phenotypes in the Shortstop and HD118-eGFP mice is differences in the *htt* transgene expression level. In comparison to endogenous htt mRNA, the Shortstop mice express the *htt* transgene ~3-fold higher than endogenous htt, whereas the YAC128 mice express htt transgene mRNA at ~3.75-fold higher than endogenous htt mRNA (42). This same study also showed that the HD-N171-82Q line 81 mice express much higher levels of transgene mRNA than either the Shortstop or YAC128 mice (42). Thus, it is quite possible that the level of expression of the N118-82Q gene in our HD118-eGFP mice is higher than that of the Shortstop mice, and the higher expression level explains the severity of the phenotype in our equivalent to the Shortstop mice. Importantly, however, we show that the HD118-eGFP mice develop abnormalities much earlier than the HD171-eGFP mice with comparable levels of mRNA expression, suggesting that the N118-82Q protein possesses greater toxicity. Given the severity of the inclusion pathology that was reported in the Shortstop mice (9), it is difficult to conclude that levels of expression alone account for the different phenotypic outcomes.

One final possibility to explain the different outcomes in our HD118-eGFP mice and the Shortstop mice is the difference in background strains of the mice that harbor the transgenes. Our HD118-eGFP mice are maintained on a B6C3F1/J background, while the Shortstop mice are on the FVB/N background. Moreover, like the Shortstop mice, premature death and weight loss are not prominent features in YAC128 and BACHD transgenic mice, which are also on the FVB/N background (26,27). Although the initial descriptions of the YAC128 mice did not indicate premature death as a phenotype, subsequent reports indicated that male YAC128 mice show slightly shortened lifespans (43). However, this phenotype was dependent upon the host strain for the transgene as breeding to C57BL/6 or 129Sv mice produced YAC128 mice with normal lifespans (44). Furthermore, *Hdh*Q111 knock-in mice backcrossed onto FVB/N, C57BL/6 or 129Sv strains showed a modulation in intergenerational and somatic instability of the polyglutamine repeat; and aggregation of mutant htt in striatum (45). Lifespan and weights were not measured in this study. Thus, there is evidence to suggest that the differences in phenotypes of our HD118-eGFP mice and the Shortstop mice might also be explained in part by differences the way the strains of mice used may regulate expression of transgenes or by differences in responses to mutant htt expression.

In summary, we demonstrate that transgenic expression of an htt fragment that is equivalent to the first two exons of htt with 82 glutamine repeats produces neurologic abnormalities similar to previously described HD mouse models. Our findings contrast the initial report of Shortstop mice described by Slow *et al*. (9), which were reported to develop inclusion pathology without neurological consequences. This report was viewed as evidence that inclusions formed by mutant htt fragment were not necessarily toxic or that short fragments of mutant htt were less toxic than full-length mutant htt. One explanation for the lack of phenotypes in the Shortstop mice was the possibility that the length of the htt fragment was critical with the shortstop fragment being less toxic than naturally derived htt N-terminal fragments (21). However, our findings suggest that this explanation is not sufficient and that other factors must be involved. The simplest explanation is that either the level or pattern of transgene expression in the Shortstop mice spared CNS structures that are critical in producing the phenotypes seen in other transgenic mouse models of HD based on expression of mutant N-terminal fragments of htt.

MATERIALS AND METHODS

All animal experiments described were approved by the University of Florida Institutional Animal Care and Use Committee. Mice were kept on a 14 h:10 h light to dark ratio and had *ad libitum* access to food and water.

Generation of transgenic mice

All transgenic mice were produced by injecting transgene vectors into single cell embryos produced by mating F1 C57Bl/6J x C3He/J mice. All lines of transgenic mice were maintained by mating male transgene positive mice with female NTg F1 C57Bl/6J x C3He/J mice.

The *htt* cDNA genes were expressed from the MoPrP.Xho vector, which has previously been described (32). The Mo.PrP-htt-N171-82Q vector has been previously described (8). To make the N118-82Q cDNA, a GC-RICH polymerase chain reaction (PCR) system (Roche, Indianapolis, IN, USA) was used to amplify DNA from an *htt*-N171-82Q cDNA template. Primers had *Xho*I restriction sites (underlined) engineered to flank the amplified cDNA: PrP-Xho/ATG-S, 5′-CGCTCGAGCCACCATGGCGACC-3′; Htt-N119Z-AS, 5′-GCCTCGAGTTATCTGACAGACTGT-3′. The PCR product was blunted with Klenow enzyme (New England Biolabs, Ipswich, MA, USA), ligated into pBluescript vector and then excised by *Xho*I and subcloned into the *Xho*I site of the MoPrP.Xho vector. The N118-82Q coding region was sequenced at the University of Florida Interdisciplinary Center for Biotechnology Research to confirm codons and number of glutamines.

The Keratin14-eGFP expression vector (Supplementary Material, Fig. S1) was made by amplifying the Keratin14 promoter from pG3Z-K14 (a generous gift from Elaine Fuchs, Rockefeller University) using the following primers: 5′-CCGGATCCGCGGCCGCCTCCGGAGCTTCTATTCC-3′ and 5′-CCGGATCCTAAATTGGAAAGGGATGCGAGTG C-3′. The 2 kb amplicon was digested with *Bam*HI (underlined sequence) and ligated into the PrP-Tet promoter vector, which is a variation of the MoPrP.Xho vector in which the PrP promoter elements have been replaced by the tetracycline operator as previously described (29). The tetracycline operator is flanked by *Bam*HI restriction sites, allowing for easy excision and replacement. Orientation of the K14 promoter was verified by sequence analysis. The eGFP cDNA was excised from its vector (Clontech #6086-1, Accession #U55761) and ligated into the *Xho*I cloning site of the new K14.PrP.Xho vector.

Genotyping

Genomic DNA was extracted from tail biopsies and used to confirm integration of the PrP-N118-82Q transgene. Approximately 200 ng of genomic DNA was amplified with the following primers in one reaction: PrP-SJ, 5′-GGGACTATGT GGACTGATGTCGG-3′; PrP-ASJ, 5′-CCAAGCCTAGACC ACGAGAATGC-3′; Htt-78-79 SmaI-S, 5′-CCACCCGGGCC GGCTGTGGCT-3′. The primer pair PrP-SJ and PrP-ASJ amplifies the endogenous PrP allele (∼750 bp) and the primer pair Htt-78-79 SmaI-S and PrP-ASJ amplifies the *htt* transgene (∼120 bp). eGFP can be detected by eye in live mouse skin with the use of an excitation lamp (FHS/LS-1B, BLS Ltd., Budapest, Hungary) affixed to filtered goggles (FHS/EF-2G2, BLS Ltd.). In the initial screening of lines, the relative levels of eGFP observed correlated with the relative ratio of *htt* transgene to endogenous PrP genes as judged by the relative abundance of PCR products from genotyping of tail DNA. To demonstrate eGFP expression in skin, newborn mice were placed in a Petri dish in a Fuji imaging system (FUJIFILM Life Science, Stamford, CT, USA). One picture was taken with bright light and another with UV light. The resulting images were false-colored with flesh or green tones depending on the exposure and emission intensity.

Northern blot

Total mouse brain RNA was isolated using the TRIzol reagent (Invitrogen, Carlsbad, CA, USA). Five microgram of RNA was electrophoresed in a formaldehyde/agarose gel and transferred to Genescreen Plus membrane (PerkinElmer, Boston, MA, USA). For analysis of HD118-eGFP mice, the membranes were incubated with radiolabeled probe (Ready-To-Go DNA Labeling Beads (-dCTP), GE Amersham, Piscataway, NJ, USA) using *htt* cDNA fragment for amino acids 78–118 as a template. This template was generated by PCR using the aforementioned Htt-78-79 SmaI-S and Htt-N119Z-AS primers. For analysis of newly generated HD171-eGFP mice, the RNA blots were incubated with radiolabeled probe using sequence excised from a cDNA plasmid encoding htt amino acids 80–171 as the template.

Western blot

Tissues were harvested, weighed and homogenized in phosphate-buffered saline (PBS) with protease inhibitor cocktail (Sigma P8340, St Louis, MO, USA). Tissue homogenate was then sonicated followed by centrifugation at 16 000*g* for 5 min. Supernatant protein concentration was determined by a BCA assay (Pierce, Rockford, IL, USA). For each sample, 10 μg of the total protein was mixed with Laemmli buffer (46), loaded on 4–20% Tris-Glycine polyacrylamide gels (Invitrogen), electrophoresed and transferred to a nitrocellulose membrane. To detect eGFP expression, membranes were incubated with anti-GFP antibody (mJL-8, 1:2000, Clontech, Mountain View, CA, USA) diluted in 5% milk/PBS with 0.01% Tween-20. Bound antibodies were detected with goat anti-mouse secondary antibodies conjugated to horseradish-peroxidase followed by chemiluminescence detection on a Fuji imaging system.

For transfections, HEK293 cells were incubated with *htt* cDNAs and Lipofectamine (Invitrogen) diluted in Opti-MEM (Gibco/Introgen) following the manufacturer's protocol. After 48 h, cells were pelleted, lysed in PBS with protease inhibitor cocktail and clarified by centrifugation at 16 000*g* for 5 min. Protein concentration was determined on the supernatant and equal amounts of supernatant protein were loaded on 4–20% Tris-Glycine polyacrylamide gels followed by transfer and blotting as previously mentioned.

Immunohistochemistry

Mice were first anesthetized and then perfused with PBS. Extracted brains were fixed by incubation in 4% paraformaldehyde in PBS for >48 h at 4°C followed by incubation in 30% sucrose in PBS for >48 h at 4°C. Brains were cryosectioned at 30 μm intervals and stored in anti-freeze solution (100 mM sodium acetate pH 6.5, 1% polyvinylpyrrolidone, 40% ethylene glycol in dH_2O). Sections were then washed in PBS 3 × 5 min, heated to 90°C for 10 min in 10 mM sodium citrate and 0.01% Tween-20, washed 2 × 5 min in PBS and incubated in 5% normal goat serum (NGS) in PBS with 0.01% Tween-20. Sections were then incubated in primary antibodies diluted in blocking buffer (5% NGS + Tween-20), washed 3 × 5 min in PBS, incubated in secondary antibodies with DAPI (1:2000, Invitrogen), diluted in blocking buffer, washed 3 × 5 min and mounted on to glass microscope slides. Sections were covered with Aqua Poly/Mount (Polysciences, Inc., Warrington, PA, USA) and glass cover slips. Images were taken on an Olympus DSU-IX81 Spinning Disc Confocal Microscope or Olympus BX60 light microscope. Primary antibodies used were 2B4 (1:1000, Millipore, Boston, MA), EM48 (1:500, Millipore) and anti-ubiquitin (1:250, Dako, Carpinteria, CA, USA). Secondary antibodies used were goat anti-mouse Alexa Fluor 488 and goat anti-rabbit Alexa Fluor 568 (1:2000, Molecular Probes/Invitrogen).

SUPPLEMENTARY MATERIAL

Supplementary Material is available at *HMG* online.

ACKNOWLEDGEMENTS

We thank Rick Morimoto, Ron Kopito, Erich Wanker and Gill Bates for discussions relating to the design of these studies. We also thank Hilda Brown, Susan Fromholt, Guilian Xu, Cameron Green and Keith Crosby for advice and technical assistance.

Conflict of Interest statement. None declared.

FUNDING

This work was supported by the Huntington's Disease Society of America and the CHDI Coalition for a Cure (A.T.N.T. and D.R.B.) and the Intramural Research Program of the NIH, Center for Cancer Research, National Cancer Institute (for D.S. and L.T.). Funding to pay the Open Access publication

charges for this article was provided by SantaFe HealthCare Alzheimer's Disease Research Center.

REFERENCES

1. Walker, F.O. (2007) Huntington's disease. *Lancet*, **369**, 218–228.
2. Huntington's Disease Collaborative Research Group. (1993) A novel gene containing a trinucleotide repeat that is expanded and unstable on Huntington's disease chromosomes. *Cell*, **72**, 971–983.
3. de la Monte, S.M., Vonsattel, J.-P. and Richardson, E.P. (1988) Morphometric demonstration of atrophic changes in the cerebral cortex, white matter, and neostriatum in Huntington's disease. *J. Neuropathol. Exp. Neurol.*, **47**, 516–525.
4. Myers, R.H., Vonsattel, J.P., Stevens, T.J., Cupples, L.A., Richardson, E.P., Martin, J.B. and Bird, E.D. (1988) Clinical and neuropathologic assessment of severity in Huntington's disease. *Neurology*, **38**, 341–347.
5. DiFiglia, M., Sapp, E., Chase, K.O., Davies, S.W., Bates, G.P., Vonsattel, J.P. and Aronin, N. (1997) Aggregation of huntingtin in neuronal intranuclear inclusions and dystrophic neurites in brain. *Science*, **277**, 1990–1993.
6. Gutekunst, C.A., Li, S.H., Yi, H., Mulroy, J.S., Kuemmerle, S., Jones, R., Rye, D., Ferrante, R.J., Hersch, S.M. and Li, X.J. (1999) Nuclear and neuropil aggregates in Huntington's disease: relationship to neuropathology. *J. Neurosci.*, **19**, 2522–2534.
7. Davies, S.W., Turmaine, M., Cozens, B.A., DiFiglia, M., Sharp, A.H., Ross, C.A., Scherzinger, E., Wanker, E.E., Mangiarini, L. and Bates, G.P. (1997) Formation of neuronal intranuclear inclusions underlies the neurological dysfunction in mice transgenic for the HD mutation. *Cell*, **90**, 537–548.
8. Schilling, G., Becher, M.W., Sharp, A.H., Jinnah, H.A., Duan, K., Kotzuk, J.A., Slunt, H.H., Ratovitski, T., Cooper, J.K., Jenkins, N.A. *et al.* (1999) Intranuclear inclusions and neuritic pathology in transgenic mice expressing a mutant N-terminal fragment of huntingtin. *Hum. Mol. Genet.*, **8**, 397–407.
9. Slow, E.J., Graham, R.K., Osmand, A.P., Devon, R.S., Lu, G., Deng, Y., Pearson, J., Vaid, K., Bissada, N., Wetzel, R. *et al.* (2005) Absence of behavioral abnormalities and neurodegeneration in vivo despite widespread neuronal huntingtin inclusions. *Proc. Natl Acad. Sci. USA*, **102**, 11402–11407.
10. Wheeler, V.C., White, J.K., Gutekunst, C.A., Vrbanac, V., Weaver, M., Li, X.J., Li, S.H., Yi, H., Vonsattel, J.P., Gusella, J.F. *et al.* (2000) Long glutamine tracts cause nuclear localization of a novel form of huntingtin in medium spiny striatal neurons in HdhQ92 and HdhQ111 knock-in mice. *Hum. Mol. Genet.*, **9**, 503–513.
11. Lin, C.H., Tallaksen-Greene, S., Chien, W.M., Cearley, J.A., Jackson, W.S., Crouse, A.B., Ren, S., Li, X.J., Albin, R.L. and Detloff, P.J. (2001) Neurological abnormalities in a knock-in mouse model of Huntington's disease. *Hum. Mol. Genet.*, **10**, 137–144.
12. Menalled, L.B., Sison, J.D., Wu, Y., Olivieri, M., Li, X.J., Li, H., Zeitlin, S. and Chesselet, M.F. (2002) Early motor dysfunction and striosomal distribution of huntingtin microaggregates in Huntington's disease knock-in mice. *J. Neurosci.*, **22**, 8266–8276.
13. Cooper, J.K., Schilling, G., Peters, M.F., Herring, W.J., Sharp, A.H., Kaminsky, Z., Masone, J., Khan, F.A., Delanoy, M., Borchelt, D.R. *et al.* (1998) Truncated N-terminal fragments of huntingtin with expanded glutamine repeats form nuclear and cytoplasmic aggregates in cell culture. *Hum. Mol. Genet.*, **7**, 783–790.
14. Kim, M., Lee, H.S., LaForet, G., McIntyre, C., Martin, E.J., Chang, P., Kim, T.W., Williams, M., Reddy, P.H., Tagle, D. *et al.* (1999) Mutant huntingtin expression in clonal striatal cells: dissociation of inclusion formation and neuronal survival by caspase inhibition. *J. Neurosci.*, **19**, 964–973.
15. Trettel, F., Rigamonti, D., Hilditch-Maguire, P., Wheeler, V.C., Sharp, A.H., Persichetti, F., Cattaneo, E. and MacDonald, M.E. (2000) Dominant phenotypes produced by the HD mutation in STHdh(Q111) striatal cells. *Hum. Mol. Genet.*, **9**, 2799–2809.
16. Lunkes, A., Lindenberg, K.S., Ben Haiem, L., Weber, C., Devys, D., Landwehrmeyer, G.B., Mandel, J.L. and Trottier, Y. (2002) Proteases acting on mutant huntingtin generate cleaved products that differentially build up cytoplasmic and nuclear inclusions. *Mol. Cell*, **10**, 259–269.
17. Schilling, G., Klevytska, A., Tebbenkamp, A.T., Juenemann, K., Cooper, J., Gonzales, V., Slunt, H., Poirer, M., Ross, C.A. and Borchelt, D.R. (2007) Characterization of huntingtin pathologic fragments in human Huntington disease, transgenic mice, and cell models. *J. Neuropathol. Exp. Neurol.*, **66**, 313–320.
18. Ratovitski, T., Nakamura, M., D'Ambola, J., Chighladze, E., Liang, Y., Wang, W., Graham, R., Hayden, M.R., Borchelt, D.R., Hirschhorn, R.R. *et al.* (2007) N-terminal proteolysis of full-length mutant huntingtin in an inducible PC12 cell model of Huntington's disease. *Cell Cycle*, **6**, 2970–2981.
19. Landles, C., Sathasivam, K., Weiss, A., Woodman, B., Moffitt, H., Finkbeiner, S., Sun, B., Gafni, J., Ellerby, L.M., Trottier, Y. *et al.* (2010) Proteolysis of mutant huntingtin produces an exon 1 fragment that accumulates as an aggregated protein in neuronal nuclei in Huntington disease. *J. Biol. Chem.*, **285**, 8808–8823.
20. Hackam, A.S., Singaraja, R., Wellington, C.L., Metzler, M., McCutcheon, K., Zhang, T., Kalchman, M. and Hayden, M.R. (1998) The influence of huntingtin protein size on nuclear localization and cellular toxicity. *J. Cell Biol.*, **141**, 1097–1105.
21. Ratovitski, T., Gucek, M., Jiang, H., Chighladze, E., Waldron, E., D'Ambola, J., Hou, Z., Liang, Y., Poirer, M.A., Hirschhorn, R.R. *et al.* (2009) Mutant Huntingtin N-terminal fragments of specific size mediate aggregation and toxicity in neuronal cells. *J. Biol. Chem.*, **284**, 10855–10867.
22. Stack, E.C., Kubilus, J.K., Smith, K., Cormier, K., Del Signore, S.J., Guelin, E., Ryu, H., Hersch, S.M. and Ferrante, R.J. (2005) Chronology of behavioral symptoms and neuropathological sequela in R6/2 Huntington's disease transgenic mice. *J. Comp. Neurol.*, **490**, 354–370.
23. Carter, R.J., Lione, L.A., Humby, T., Mangiarini, L., Mahal, A., Bates, G.P., Dunnett, S.B. and Morton, A.J. (1999) Characterization of progressive motor deficits in mice transgenic for the human Huntington's disease mutation. *J. Neurosci.*, **19**, 3248–3257.
24. Mangiarini, L., Sathasivam, K., Seller, M., Cozens, B., Harper, A., Hetherington, C., Lawton, M., Trottier, Y., Lehrach, H., Davies, S.W. *et al.* (1996) Exon 1 of the *HD* gene with an expanded CAG repeat is sufficient to cause a progressive neurological phenotype in transgenic mice. *Cell*, **87**, 493–506.
25. Schilling, G., Jinnah, H.A., Gonzales, V., Coonfield, M.L., Kim, Y., Wood, J.D., Price, D.L., Li, X.J., Jenkins, N., Copeland, N. *et al.* (2001) Distinct behavioral and neuropathological abnormalities in transgenic mouse models of HD and DRPLA. *Neurobiol. Dis.*, **8**, 405–418.
26. Slow, E.J., van Raamsdonk, J., Rogers, D., Coleman, S.H., Graham, R.K., Deng, Y., Oh, R., Bissada, N., Hossain, S.M., Yang, Y.Z. *et al.* (2003) Selective striatal neuronal loss in a YAC128 mouse model of Huntington disease. *Hum. Mol. Genet.*, **12**, 1555–1567.
27. Gray, M., Shirasaki, D.I., Cepeda, C., Andre, V.M., Wilburn, B., Lu, X.H., Tao, J., Yamazaki, I., Li, S.H., Sun, Y.E. *et al.* (2008) Full-length human mutant huntingtin with a stable polyglutamine repeat can elicit progressive and selective neuropathogenesis in BACHD mice. *J. Neurosci.*, **28**, 6182–6195.
28. Woodman, B., Butler, R., Landles, C., Lupton, M.K., Tse, J., Hockly, E., Moffitt, H., Sathasivam, K. and Bates, G.P. (2007) The Hdh(Q150/Q150) knock-in mouse model of HD and the R6/2 exon 1 model develop comparable and widespread molecular phenotypes. *Brain Res. Bull.*, **72**, 83–97.
29. Jankowsky, J.L., Slunt, H.H., Gonzales, V., Savonenko, A.V., Wen, J.C., Jenkins, N.A., Copeland, N.G., Younkin, L.H., Lester, H.A., Younkin, S.G. *et al.* (2005) Persistent amyloidosis following suppression of Abeta production in a transgenic model of Alzheimer disease. *PLoS Med.*, **2**, e355.
30. Folger, K.R., Wong, E.A., Wahl, G. and Capecchi, M.R. (1982) Patterns of integration of DNA microinjected into cultured mammalian cells: evidence for homologous recombination between injected plasmid DNA molecules. *Mol. Cell Biol.*, **2**, 1372–1387.
31. Jankowsky, J.L., Slunt, H.H., Ratovitski, T., Jenkins, N.A., Copeland, N.G. and Borchelt, D.R. (2001) Co-expression of multiple transgenes in mouse CNS: a comparison of strategies. *Biomol. Eng.*, **17**, 157–165.
32. Borchelt, D.R., Davis, J., Fischer, M., Lee, M.K., Slunt, H.H., Ratovitsky, T., Regard, J., Copeland, N.G., Jenkins, N.A., Sisodia, S.S. *et al.* (1996) A vector for expressing foreign genes in the brains and hearts of transgenic mice. *Genet. Anal. (Biomed. Eng.)*, **13**, 159–163.
33. Yamaguchi, M., Saito, H., Suzuki, M. and Mori, K. (2000) Visualization of neurogenesis in the central nervous system using nestin promoter-GFP transgenic mice. *Neuroreport*, **11**, 1991–1996.

34. Zong, H., Espinosa, J.S., Su, H.H., Muzumdar, M.D. and Luo, L. (2005) Mosaic analysis with double markers in mice. *Cell*, **121**, 479–492.
35. Livet, J., Weissman, T.A., Kang, H., Draft, R.W., Lu, J., Bennis, R.A., Sanes, J.R. and Lichtman, J.W. (2007) Transgenic strategies for combinatorial expression of fluorescent proteins in the nervous system. *Nature*, **450**, 56–62.
36. Hodgson, J.G., Agopyan, N., Gutekunst, C.A., Leavitt, B.R., LePiane, F., Singaraja, R., Smith, D.J., Bissada, N., McCutcheon, K., Nasir, J. *et al.* (1999) A YAC mouse model for Huntington's disease with full-length mutant huntingtin, cytoplasmic toxicity, and selective striatal neurodegeneration. *Neuron*, **23**, 181–192.
37. Zeitlin, S., Liu, J.-P., Chapman, D.L., Papaioannou, V.E. and Efstratiadis, A. (1995) Increased apoptosis and early embryonic lethality in mice nullizygous for the Huntington's disease gene homologue. *Nat. Genet.*, **11**, 155–163.
38. Bhide, P.G., Day, M., Sapp, E., Schwarz, C., Sheth, A., Kim, J., Young, A.B., Penney, J., Golden, J., Aronin, N. *et al.* (1996) Expression of normal and mutant huntingtin in the developing brain. *J. Neurosci.*, **16**, 5523–5535.
39. Manson, J., West, J.D., Thomson, V., McBride, P., Kaufman, M.H. and Hope, J. (1992) The prion protein gene: a role in mouse embryogenesis? *Development*, **115**, 117–122.
40. Yamamoto, A., Lucas, J.J. and Hen, R. (2000) Reversal of neuropathology and motor dysfunction in a conditional model of huntington's disease. *Cell*, **101**, 57–66.
41. Weydt, P., Pineda, V.V., Torrence, A.E., Libby, R.T., Satterfield, T.F., Lazarowski, E.R., Gilbert, M.L., Morton, G.J., Bammler, T.K., Strand, A.D. *et al.* (2006) Thermoregulatory and metabolic defects in Huntington's disease transgenic mice implicate PGC-1alpha in Huntington's disease neurodegeneration. *Cell Metab.*, **4**, 349–362.
42. Wang, C.E., Tydlacka, S., Orr, A.L., Yang, S.H., Graham, R.K., Hayden, M.R., Li, S., Chan, A.W. and Li, X.J. (2008) Accumulation of N-terminal mutant huntingtin in mouse and monkey models implicated as a pathogenic mechanism in Huntington's disease. *Hum. Mol. Genet.*, **17**, 2738–2751.
43. Van Raamsdonk, J.M., Pearson, J., Rogers, D.A., Bissada, N., Vogl, A.W., Hayden, M.R. and Leavitt, B.R. (2005) Loss of wild-type huntingtin influences motor dysfunction and survival in the YAC128 mouse model of Huntington disease. *Hum. Mol. Genet.*, **14**, 1379–1392.
44. Van Raamsdonk, J.M., Metzler, M., Slow, E., Pearson, J., Schwab, C., Carroll, J., Graham, R.K., Leavitt, B.R. and Hayden, M.R. (2007) Phenotypic abnormalities in the YAC128 mouse model of Huntington disease are penetrant on multiple genetic backgrounds and modulated by strain. *Neurobiol. Dis.*, **26**, 189–200.
45. Lloret, A., Dragileva, E., Teed, A., Espinola, J., Fossale, E., Gillis, T., Lopez, E., Myers, R.H., MacDonald, M.E. and Wheeler, V.C. (2006) Genetic background modifies nuclear mutant huntingtin accumulation and HD CAG repeat instability in Huntington's disease knock-in mice. *Hum. Mol. Genet.*, **15**, 2015–2024.
46. Laemmli, U.K. (1970) Cleavage of structural proteins during the assembly of the head of bacteriophage T4. *Nat. (Lond.)*, **227**, 680–685.